RPN3

SC-RR-69-421

SUMMARY OF THE HERMES FLASH X-RAY PROGRAM

T. H. Martin, 5245
K. R. Prestwich, 5245
D. L. Johnson, 5245

October 1969

ABSTRACT

The Hermes program produced significant information in the areas of Marx generator design, flash x-ray tube development, dielectric breakdown, and general flash x-ray machine design. As an outcome of the Hermes program, Hermes II was constructed and is the largest flash x-ray machine presently operating. This report summarizes the results of investigations in the areas mentioned and provides a general knowledge in the operation of megavolt flash x-ray machines which should be useful to the experimenters using these machines.

ACKNOWLEDGMENT

Portions of the work presented here are the result of the combined efforts of members of the Radiation Source Research Division. In particular the authors wish to thank D. A. Butel for his structural analysis and mechanical design on both Hermes I and Hermes II; J. E. Boers for his computer solutions; and R. S. Clark for performing many of the experiments and for his contributions in component design.

TABLE OF CONTENTS

SUMMARY OF THE HERMES FLASH X-RAY PROGRAM

INTRODUCTION

As a result of the rapid growth of pulsed power technology during the last decade, attributable in part to research performed by the Atomic Weapons Research Establishment (AWRE), Sandia Laboratories has developed, fabricated, and is operating Hermes II, the largest flash x-ray machine presently available. Hermes II has produced a 150-kA beam of electrons at energies of 12 million volts for times of 100 nsec.

Hermes I, a one-tenth scale model of Hermes II, was constructed to perform necessary experimentation for the development of Hermes II. In this report the design and performance of the Hermes II together with appropriate data from Hermes I is reviewed. Hermes I was later used as an operational electron beam facility.

GENERAL DESCRIPTION

The Hermes machines utilize accelerator principles described in the literature.[1-6] The component parts are a low-inductance Marx generator, a Blumlein transmission line,[7] and a vacuum tube in which the electron beam is formed by field emission and accelerated across the cathode-anode region by means of an applied voltage. All high-voltage portions of the generator are submerged in transformer oil for insulation.

The Hermes II components are housed in a steel cylinder 85 feet long and 22 feet in diameter which contains approximately 150,000 gallons of oil. Hermes II is shown in Fig. 1.

The Marx generator was designed as an 18-MV, 1-MJ generator and has been operated to 11 MV and 0.5 MJ. It is composed of 186 capacitor stages, each stage consisting of two 1/2-μF, 100-kV capacitors in

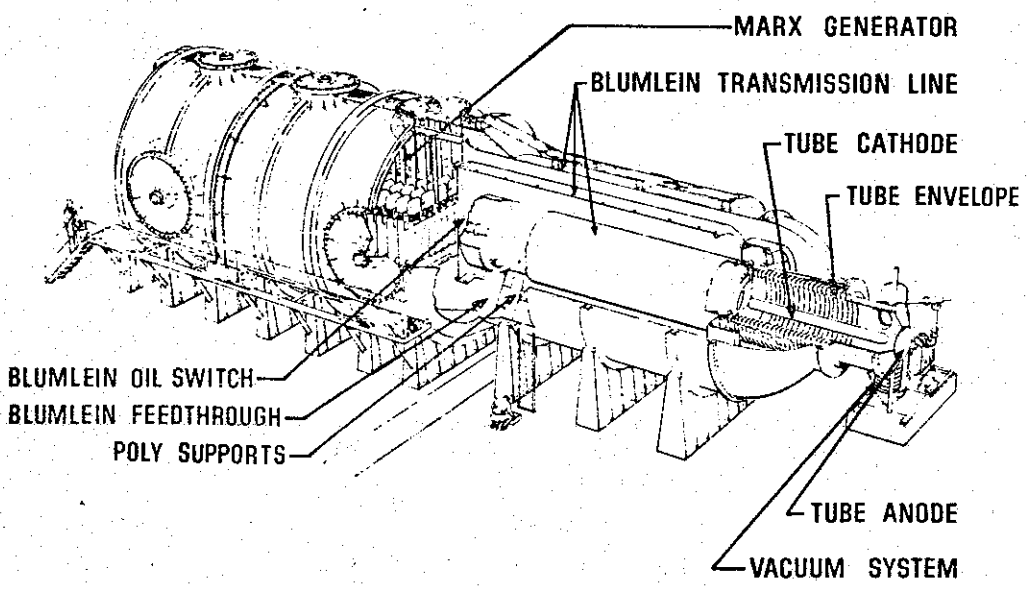

Fig. 1 Hermes II.

parallel. The geometrical arrangement of the capacitors takes advantage of the stray capacities to provide a wide triggering range and fast erection time. The total system inductance is 80 μH, which permits transfer of the energy from the Marx generator to the Blumlein in 1.5 μsec.

The outer Blumlein cylinder is 16 feet in diameter and forms a 12-Ω output impedance for the outer line and an inner line impedance of 22 Ω. The output impedance of the Blumlein is 34 Ω. The electrical length is 87 nsec with a total capacity of 5.2 nF.

Choice of the relative diameters of the Blumlein was governed by making the maximum electric field in each of the transmission lines equal and maximizing the bremsstrahlung output for a given Marx charge voltage.

The Hermes II vacuum tube envelope approximates those referenced in the literature.[8] The 48-inch-diameter lucite tube has been tested in two lengths, 72 and 88 inches. An epoxy tube 78 inches in diameter and 96 inches long was also used successfully.

MAJOR RESEARCH AREAS

Marx Generator Circuitry

Marx generators have been used to generate voltages up to 2 MV for impulse testing of dielectric breakdown for many years.[9] The peak voltages and energy storage of Marx generators have been significantly increased by the development of multimegavolt flash x-ray machines.[4-6] The Hermes II Marx generator is presently the highest voltage, largest energy storage unit operating in a flash x-ray machine.

Voltage multiplication is accomplished in Marx generators by charging capacitors in parallel and discharging them in series. Spark gaps are generally used to switch from the parallel to the series arrangement. Usually one or two of the gaps are triggered and the remainder are overvolted by the transient voltages within the generator. Proper stage-to-stage capacitive or resistive coupling must be maintained to insure that the untriggered spark gaps will be overvolted.[9,10] The simple Marx circuit shown in Fig. 2 can be used to explain capacitive and resistive coupling. Stray capacities are indicated by dashed lines.

The capacitors can be arranged in such a manner that the stray capacity (C_R) between alternate stages is large. These stages are connected with charging resistors. If gaps (1) and (2) in Fig. 2 are triggered, point A becomes clamped at V_o and point B at 3 V_o. The voltage at point D will be determined initially by voltage division among the stray capacities. If this is a long generator and the capacity to ground from every capacitor is small compared to C_R, the voltage across gap (3) becomes approximately 2 V_o $C_R/(C_R + C_g)$. The voltage across C_R decays to zero with a time constant of $R(C_R + C_g)$, and the voltage across gap (3) then approaches 2 V_o. Since the voltage across each gap approaches twice its dc value, the Marx generator is called an n = 2 generator. An n = 2 generator can be triggered down to nearly 50 percent of the self-breakdown voltage (V_B) of the spark gaps. Similarly, if the coupling is such that the voltage across the spark gaps approaches pV_o, the generator is called an n = p generator and it would trigger down to 100/p percent of V_B.

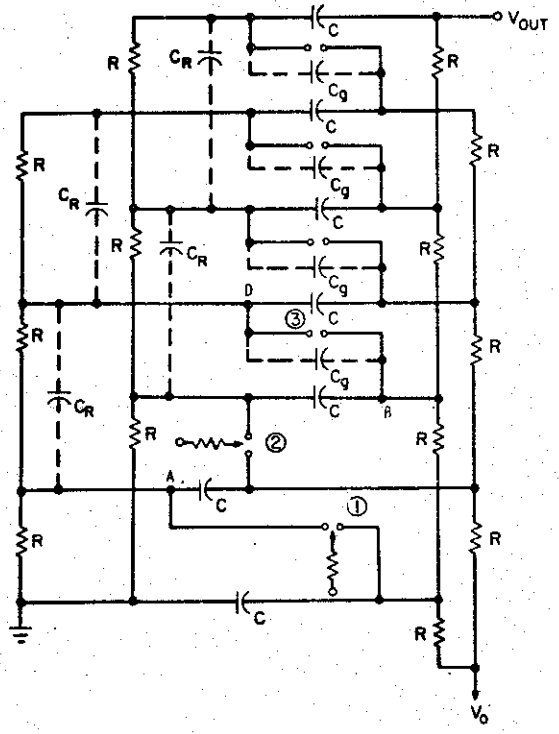

Fig. 2 n = 2 Marx generator.

It is also possible to arrange the components in such a way that the capacitive coupling is X and the resistive coupling is Y. In this case the voltage across the spark gaps caused by the capacitive division will become $XV_oC_R/(C_R + C_g)$ immediately. The charge resistors are coupled across Y stages and C_R would discharge to give YV_o across the the spark gaps.

To gain a more thorough knowledge of the operation of Marx generators with many stages, several model Marx generators were constructed. A capacitor arrangement was sought that would trigger over a large voltage range for any given spark gap setting, that would switch very rapidly, that could be easily assembled and maintained when constructed with 1/2-μF, 100-kV capacitors, and that would have a reasonably low inductance. The Marx models were constructed with 10-kV, 1/4-μF capacitors. The effects of varying the value of charging resistors and stray capacities were investigated.

Figures 3 and 4 are schematic diagrams of two generators studied. The diagrams indicate the mechanical arrangement of the capacitors and resistors. By charging half of the capacitors to plus V_o and half to minus V_o, the required number of spark gaps is halved.

F3 &

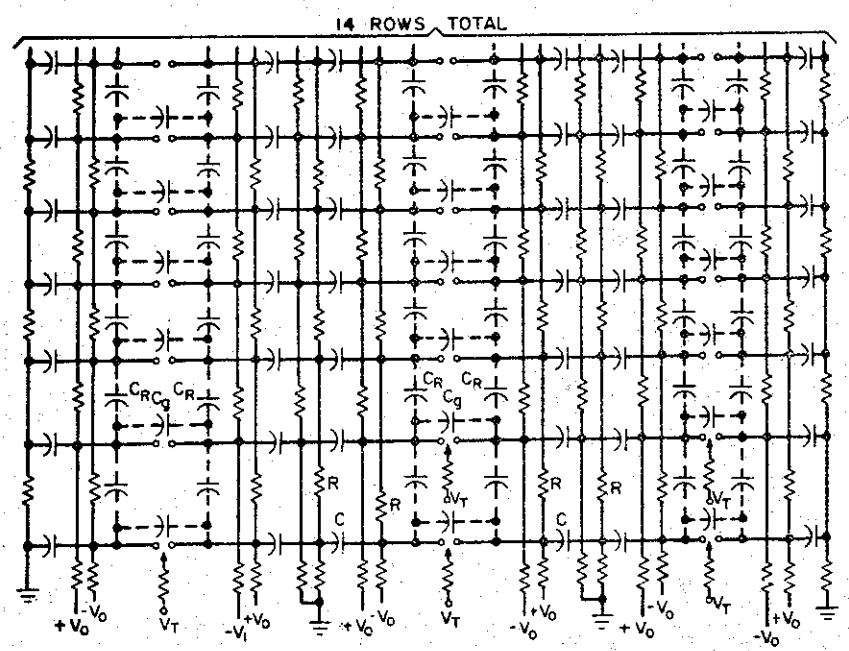

Fig. 3 Type S Marx generator.

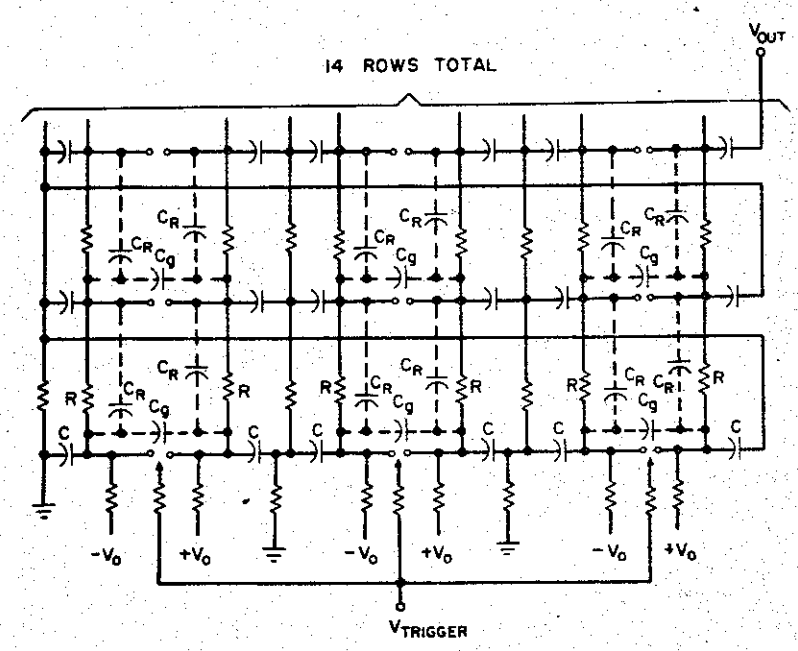

Fig. 4 Type Z Marx generator.

The type S Marx generator (Fig. 3) has capacitive coupling that varies from n = 1 to n = 5 across the generator. The resistive coupling is n = 6 after the first six gaps have fired, but varies from n = 2 to n = 5 if one to five gaps have fired. If 3 gaps were triggered, the minimum trigger voltage was 50 percent of V_B. If 5 gaps were triggered, the minimum trigger voltage was 26 percent of V_B. The minimum firing voltage was not affected by locating the triggered gaps at different points in the generator if 3 or 5 adjacent gaps were triggered. This layout has the lowest inductance of any of those considered.

The type Z (Fig. 4) generator has n = 3 resistive and capacitive coupling. If 3 gaps were triggered, it would fire down to 30 percent of V_B. Triggering 5 gaps did not increase the firing range. If the resistors were connected in n = 6 configuration and 5 gaps triggered, the generator would run at 20 percent of V_B. The inductance of this generator was measured to be 69 μH.

Figure 5 is a plot of switching time versus the fraction 2 V_o/V_B for both the S and Z Marx generators, where 2 V_o is the dc voltage applied across each spark gap. F5

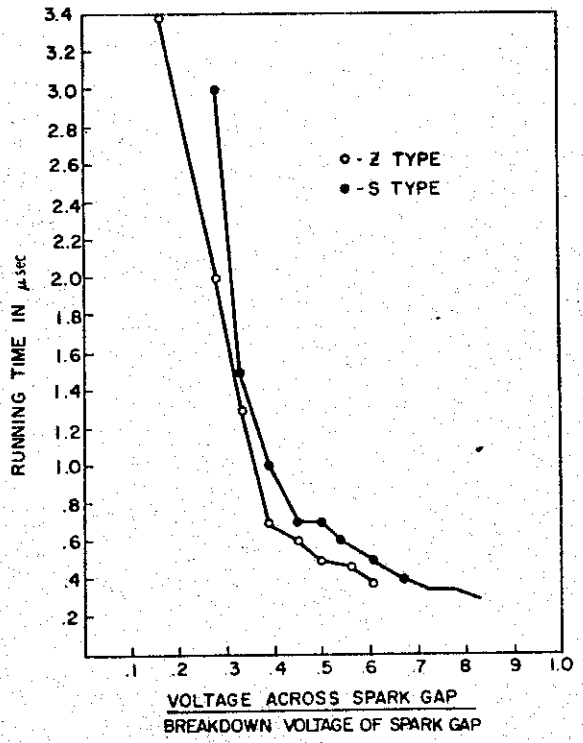

Fig. 5 Switching times for model Marx generators.

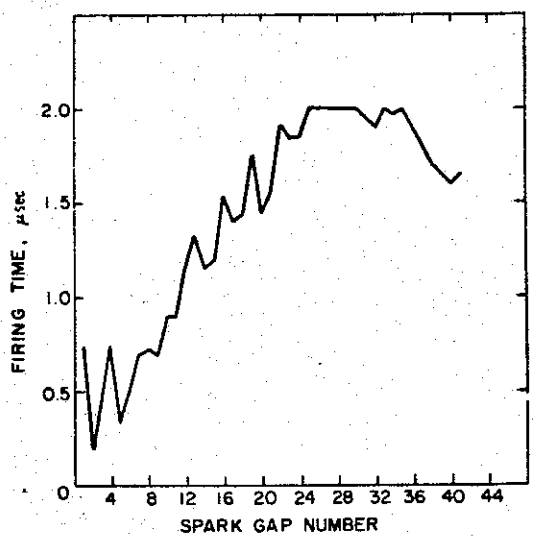

Fig. 6 Gap breakdown versus time.

Streak photographs of the Z Marx were taken to show the firing-time sequence of the spark gaps. Figure 6 is a plot of relative breakdown times of each gap taken from one of the streak photographs. The gaps are numbered sequentially from the ground end with gaps 1, 2, and 3 the triggered gaps. An interesting point is that after 23 gaps had broken down, the gaps from the high-voltage end began to fire sequentially and, finally, the last seven gaps broke down simultaneously.

4-MV Marx Generator

Since model studies indicated that the n = 3 type Z Marx generator would fire at a reasonably low voltage, had good running characteristics, low inductance, and would simplify construction and maintenance problems, this layout was chosen for the Hermes II Marx generator. To further model the operation of this type of Marx generator, a 4-MV, 100-kJ generator was constructed. The capacitors, spark gaps, resistors, and support structure proposed for the 18-MV generator were used. This Marx generator is the energy storage system for Hermes I.

Figure 7 is a scaled drawing of one row of the Hermes I generator. The generator consists of six complete rows and one partial row to provide electrical grading on the high-voltage end. There is a 6-inch separation between rows of the 8-inch-diameter capacitors. A copper

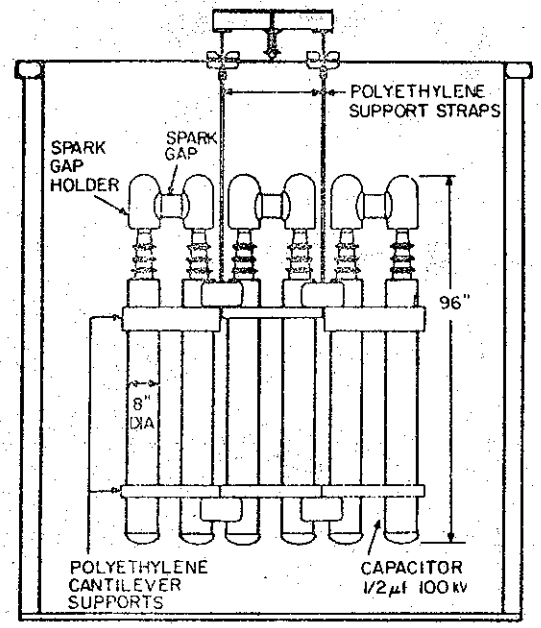

Fig. 7 One row of Hermes I Marx generator.

screen located 24 inches above the spark gap holders and below the surface of the transformer oil covers the Marx generator. The 1- x 4-inch polyethylene straps are attached to the capacitors in a low electric field area. Figure 8 is a photograph of the complete Marx generator before installation in its steel tank (10 ft wide by 12 ft long by 12 ft high) and immersion in transformer oil. The copper sulphate charge resistors are constructed with vinyl tubing housings and copper tubing terminals. The charge resistors and ground resistors are 1.2 kΩ and 25 kΩ between each row, respectively. These resistors, together with the series resistance inherent in the Marx, discharge the generator with a 16-μsec time constant. The spark gaps are individually housed, since analysis indicated that ultraviolet coupling between gaps was not necessary in this type of generator.

The generator has 22-μH inductance, 13.1-nF series capacitance, and 4-Ω series resistance. It charges a triaxial Blumlein transmission line to peak voltage in 0.75 μsec. Since the capacity of the transmission line is smaller than the capacity of the generator, an inductive ringing gain exists. The peak output voltage of the generator has been 4.5 MV. An oil spark gap in the transmission line grounds the Marx through an inductor when full voltage is achieved on the transmission line. The generator then oscillates and is damped out by its parallel and series resistance. Peak charge currents are 35 kA and peak ringing

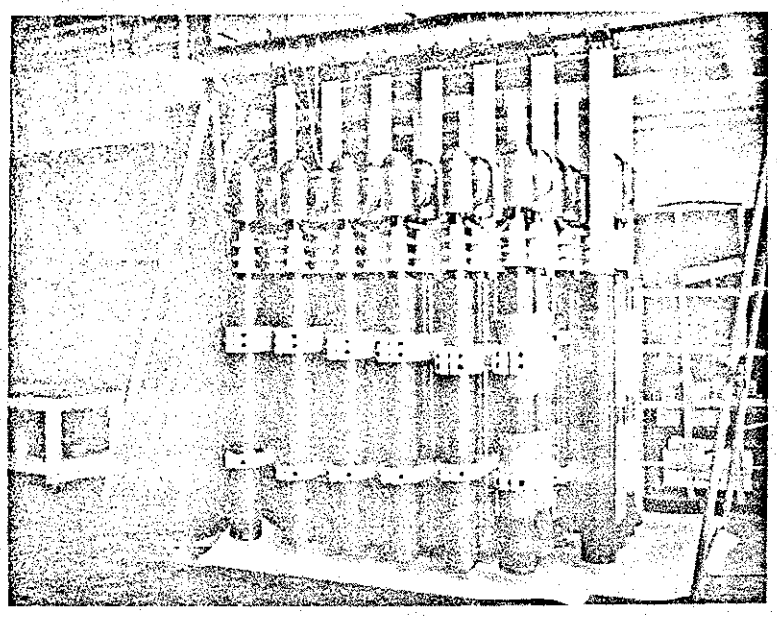

Fig. 8 Hermes I Marx generator.

currents 70 kA. The generator has operated for over 5000 shots with only minor maintenance. The capacity C_g (see Fig. 4) is estimated to be 45 pF, C_R is approximately 90 pF, and the strays from each stage to ground are less than 20 pF. The first approximation indicates that capacitive division would immediately increase the gap voltage to 4 V_o, and resistive coupling would increase it to 6 V_o with a time constant of about 0.15 μsec. The Marx generator is usually operated with V_o equal to $V_B/3$. Therefore, the gap voltage increases to 1.2 V_B immediately and continues to increase toward 1.8 V_B until breakdown occurs. The generator has operated down to 41 percent of V_B.

18-MV Marx Generator

The 18-MV Marx generator developed for Hermes II is similar to that for the Hermes I except that each stage consists of two 1/2-μF, 100-kV capacitors in parallel. The cantilever supports (see Fig. 7) were modified to increase the arc tracking length and the polyethylene support straps were increased to 8 inches width. There are 186 capacitor stages and 93 spark gaps in 31 rows. The generator is immersed

in transformer oil contained in a 40-foot steel tank having a 20-foot inside diameter. The shortest distance from the Marx generator to the tank wall is 4 feet.

When the capacitors are charged to 103 kV, the generator stores 1 MJ of energy. Its series capacity is 5.38 nF and it charges a 5.2-nF transmission line. The calculated inductance and series resistance are 80 μH and 20 Ω. The charge resistors are 1.5 kΩ per section and will discharge the generator with a time constant of 25 μsec. The transmission line is charged in 1.5 μsec. With these parameters the Marx generator could charge the transmission line to 16.3 MV. At the present time the capacitors have been charged to 73 kV (1/2 MJ energy storage), which placed 11 MV on the Blumlein.

In this generator, C_g (see Fig. 4) is estimated to be 45 pF, C_R is 190 pF, and the capacity per stage to ground is less than 10 pF. Therefore, capacity coupling would increase the voltage across the spark gap to 4.9 V_o immediately. It would further increase to 6 V_o with a time constant of 0.3 μsec. The generator will fire down to 40 percent of V_B.

Spark Gaps

Pressurized, individually housed spark gaps are used to switch the Hermes' Marx generators. A gap, shown in Fig. 9, has a self-breakdown voltage characteristic as shown in Fig. 10 if dry air is used for the gas dielectric.

With the use of an electrolytic tank plotter the shapes of the electrode, electrode holder, and spark gap holder were determined so that the electric field was constant over a 1.5-inch-diameter circle in the center of the electrode and would fall off gradually at the edges. Nylon was chosen as a housing material because of its strength, machinability, and resistance to surface arcing (tracking).

Tests to determine a suitable electrode material were performed by discharging an L-C circuit of 2.4 μH and 1.25 μF charged to 180 kV through the spark gap. Peak currents of 130 kA were produced in a

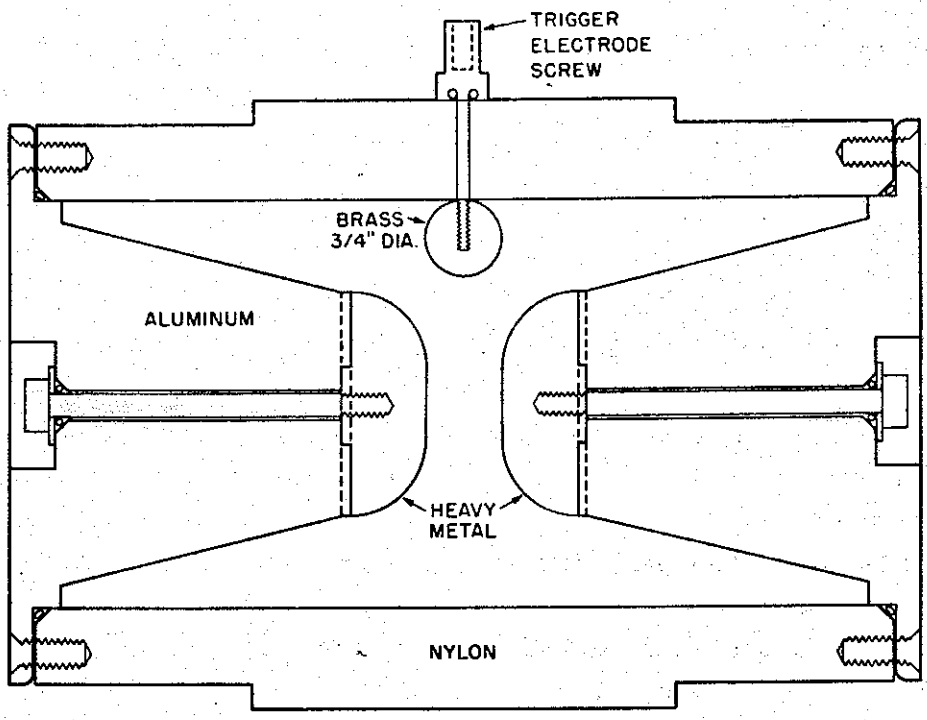

Fig. 9 Hermes spark gap.

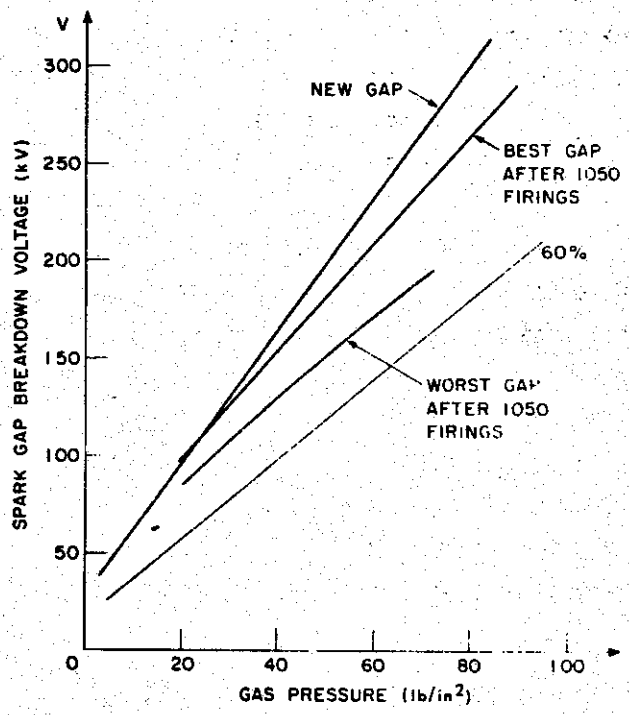

Fig. 10 Hermes spark gap breakdown characteristics.

sinusoidal waveform having a 10-μsec period and a decay time constant of 45 μsec. A dry nitrogen fill gas was used at a constant pressure and the capacitors were charged and then discharged by the self-breakdown of the gap. This process was repeated until the voltage holdoff was reduced to 60 percent of its original value. Brass, chrome, and stainless steel electrodes were good for only three discharges, while molybdenum electrodes were good for seven discharges. A tungsten-copper-nickel alloy, commonly called heavy metal (Fansteel 77), was tested for 59 discharges. The breakdown voltage decreased to 74 percent of its original value for a gas pressure of 60 lb/in.^{2} The gas pressure was changed to 100 lb/in.^{2} for the same number of discharges and the breakdown voltage changed to 63 percent of its original value. This test simulated the peak current of an early Marx generator design, but on a subsequent modification it was more severe than necessary. It was felt that a better test would be to match, for the test circuit and Marx generator, the sum of the product of the current times the charge transferred in each half-cycle until the current was 1/e of its original value.[10]

Spark gap lifetime tests with heavy metal electrodes were performed with the use of the electrode materials test circuit. Triggered spark gaps were used to insure that breakdowns occurred at a constant voltage regardless of electrode damage. Two fill gases were tested: dry nitrogen and dry air (21 percent oxygen, 79 percent nitrogen). Periodic sampling of the gap breakdown voltage was made with a low-current power supply. Test results of 300 firings at 120 kV and 55 lb/in.^{2} air pressure on the gaps are shown in Fig. 11. Gaps with dry air as a fill gas showed less electrode damage and a smaller variance in breakdown voltages than those tested using dry nitrogen. Dry air is now utilized as the spark gap fill gas for the Hermes machines.

After 1050 firings of Hermes I, eleven of the spark gaps were removed and tested for breakdown voltage on a low-current power supply. The results of these tests are tabulated in Table 1 and shown in Fig. 10. Table 2 gives the percentage of the 1050 firings for several ranges of spark gap voltage. The approximate peak currents are given in this table.

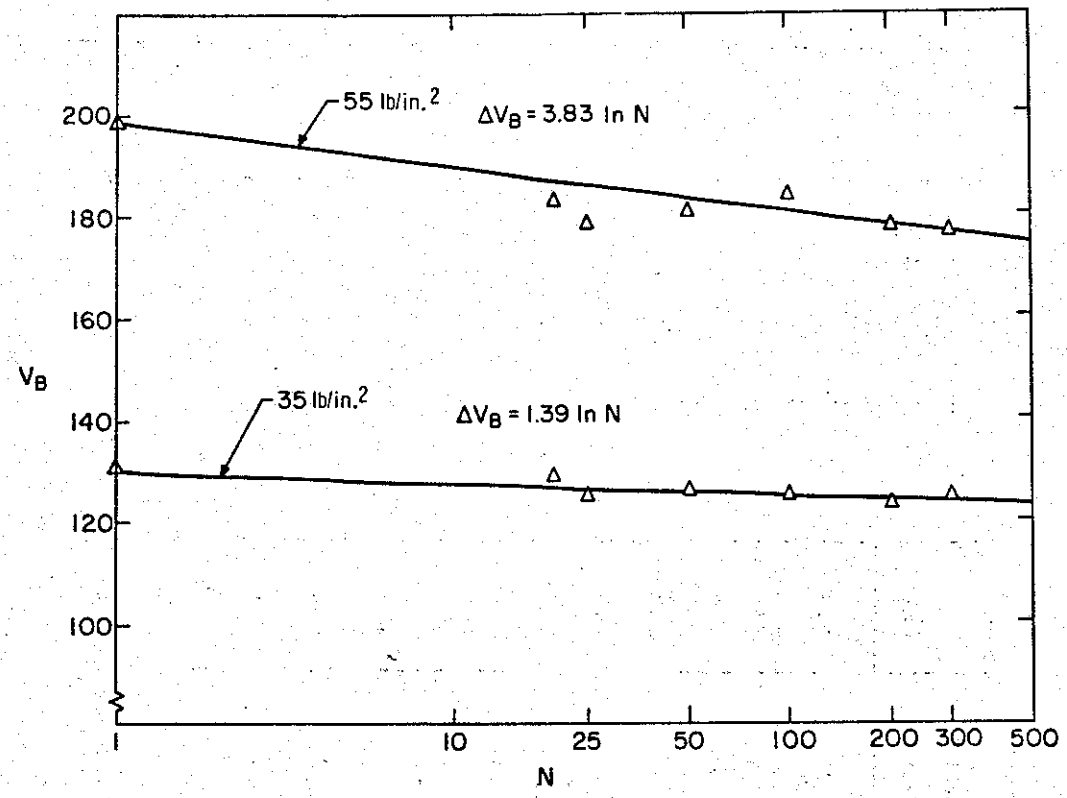

Fig. 11 Spark gap breakdown voltage versus number of firings.

Some of the electrodes were damaged uniformly over the constant stressed electrode area, while others were damaged only at one small spot. The degradation of the breakdown voltage for the small spot gaps was considerably worse than for the other gaps. Gap numbers 2, 3, 4, 8, and 10 in Table 1 were small spot gaps and numbers 7, 9, and 11 were uniform breakdowns.

The AWRE performed life test experiments on this type of spark gap and found that stainless steel performed better than heavy metal.[11] One set of stainless steel electrodes was tested for 191 shots in Hermes I and the breakdown strength degraded 8 percent. Two other sets of electrodes were tested in Hermes I. One set of the electrodes was heavy metal and the other was stainless steel. These were checked after 300 firings on a modified Hermes I which left less energy in the Marx generator after the Blumlein switch closed. There was no degradation of the voltage breakdown values of either set of electrodes.

TABLE 1

HERMES I Spark Gap Breakdown Voltage After 1050 Firings

	40 psi			60 psi			70 psi		
Gap number	$\bar{V}_B$ (kV)	Percent decrease†	σ (kV)	$\bar{V}_B$ (kV)	Percent decrease†	σ (kV)	$\bar{V}_B$ (kV)	Percent decrease†	σ (kV)
1	147	10.3	3.5	191	18.0	8.4	211	19.4	12.2
2	136	17.0	5.9	176	24.4	5.9	205	21.8	4.1
3	138	15.8	5.4	178	23.6	4.4	204	22.1	2.5
4	135	17.7	4.1	170	27.0	6.2	192	26.7	6.6
5	147	10.3	4.6	192	17.6	7.9	214	18.3	12.8
6	142	13.4	4.6	186	20.0	3.7	205	21.8	11.3
7	154	6.1	1.3	210	9.9	2.2	-	-	-
8	134	18.3	3.8	166	28.7	2.2	189	27.8	1.5
9	145	11.6	2.8	198	15.0	1.4	-	-	-
10	131	20.0	3.0	174	25.3	4.7	199	24.0	3.7
11	149	9.1	2.5	196	15.9	4.8	212	19.1	10.0
12*	164	-	2.1	233	-	1.9	262	-	2.5

*Number 12 is a typical new gap; σ will vary some from gap to gap when the gaps are new.

†Percent decrease $= \dfrac{\bar{V}_{B_{new}} - \bar{V}_B}{\bar{V}_{B_{new}}} (100)$.

TABLE 2

Percentage of 1050 Firings for Several Ranges of Spark Gap Voltage

Spark gap voltage (kV)	Percent of firings	Maximum first cycle current (kA)	Maximum ringing current (kA)
< 60	19	10.4	18.4
61-80	37	13.9	24.6
81-100	20	17.3	30.7
101-120	11	21.0	37.0
121-140	6	24.0	43.0
141-160	4	28.0	49.0
161-180	2	31.0	55.0
> 180	1	35.0	61.0

Hermes II spark gaps are identical to those used in Hermes I. Several gaps in Hermes II have tracked internally. Three gaps in Hermes I and one in Hermes II have tracked on the outside of the gap from the trigger terminal to the positive electrode, causing mechanical failure of the gap. This problem was easily corrected by modification of the trigger terminal.

Based on information gained in developing and operating these generators, it is probable that even higher voltage Marx generators could be constructed with little difficulty. The inductance per stage of the Marx generator could be reduced by using lower inductance capacitors and arranging them in some combination of S and Z Marx generators. Since the spark gaps could operate with a substantial increase in current, Marx generators with higher energy storage could also be constructed by increasing the capacity per stage.

Oil Dielectric Data

The oil breakdown data utilized for the original designs were generated by AWRE and have not been published formally.[10] It was demonstrated by the AWRE group that uniform field voltage breakdown levels of oil depend on time, electrode area, and applied field. The AWRE-generated curve showing these effects is shown in Fig. 12. The peak electrical field, F, is in megavolts per centimeter, t is in microseconds and is defined as the time during which the voltage exceeds 63 percent of its peak voltage, and area is in cm^2.

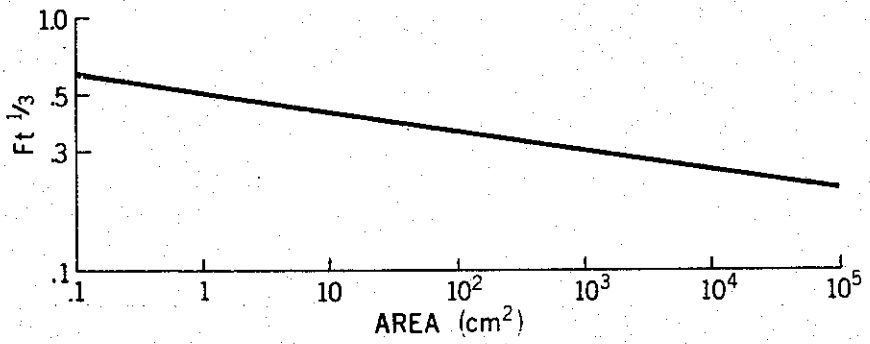

Fig. 12 Pulsed breakdown data for transformer oil.

In nonuniform fields it has been shown that breakdown voltage stresses of the negative electrode are appreciably higher than those of the positive electrode. Subsequently, the negative electrode can be stressed to higher levels before breaking. The ratio between the negative and positive breakdown level is known as the polarity factor.

At the beginning of the Hermes program, the largest area oil breakdown data point was at 10^4 cm^2. This is less than the combined area of 3.4×10^6 cm^2 of the Hermes II Blumleins. A tabulation of the presently achieved levels of oil stress of the Hermes program is shown in Table 3. It should be emphasized that these are the maximum voltage levels obtained on the Hermes program; breakdowns did not occur at these levels.

TABLE 3

Dielectric Stress of Transformer Oil
in Hermes Blumleins

Machine cylinder	Maximum applied voltage (MV)	Electric field (MV/cm)	Area (cm^2)	$F\ t^{1/3}$
Hermes II:	effective time, 0.52 μsec			
Inner*	+11	0.21	4.7×10^5	0.17
Inter.	-11	0.20	9.0×10^5	0.16
Outer	+11	0.15	1.2×10^6	0.12
Hermes I:	effective time, 0.27 μsec			
Inner	+4.5	0.24	6.4×10^4	0.15
Inter.	-4.5	0.23	1.6×10^5	0.15
Outer	+4.5	0.17	2.0×10^5	0.11
Hermes I:	effective time, 0.33 μsec			
Inner*	+3.4	0.24	2.5×10^5	0.17
Inter.*	-3.4	0.25	3.3×10^5	0.17
Outer	+3.4	0.21	4.0×10^5	0.15

*Coated with 9300 Series of Rust Oleum epoxy paint.

Oil breakdowns have occurred in Hermes II between the feedthrough to the center Blumlein cylinder and its associated hole in the intermediate cylinder and represent a design problem of the Blumlein-type machine. This location can be seen in Fig. 1. At 10.8 MV, an arc occurred between the 3-inch-diameter pipe at the hole edge to the 26-inch-diameter feedthrough pipe. The maximum field was calculated to be 0.66 MV/cm over a stressed area of 2×10^3 cm^2 and an effective time of 0.50 μsec. In comparison of this point with the above data, a polarity and nonuniformity factor of 1.86 was determined for this configuration.

The edges of the feedthrough hole were then lined with 8-inch-diameter pipe to reduce the dielectric stress, and the experiment was repeated. At 10.4 MV, a feeble arc occurred from the positive cylinder to the new lines and, with a stressed area of 1.4×10^4 cm^2, F $t^{1/3}$ was calculated to be 0.24 as compared to 0.26 from the AWRE oil breakdown curve. Detailed oil breakdown data were obtained from the Hermes II oil switch. The Hermes II Blumlein oil switch operates with an average dielectric stress of 0.43 MV/cm (σ = 0.5 MV/cm, maximum stress 0.53, minimum stress 0.32, and average F $t^{1/3}$ = 0.32) over an area of 100 cm^2.

Polyethylene Supports

Polyethylene was used as the material to support the Marx generator and the Blumlein. Each of the 31 rows in the Marx generator is hung by two polyethylene hanger straps, nominally 5 feet long, attached between the capacitor cases and the top of the containing tank.

During 740 firings of the machine with voltages in the 7- to 11-MV range, arcs occurred on the surface of five of these straps. The surface arcs did not cause mechanical failure of the straps.

One of the 12-inch-diameter high density polyethylene supports in the Blumlein section (shown in Fig. 1) failed at a level of 11 MV, or a maximum field strength of 0.21 MV/cm. After replacement of the support, the Blumlein was then charged to voltages exceeding 10 MV six times without further failure. Experience indicates that 0.21 MV/cm is near the limiting working stress for this insulator.

Tube Insulator Characteristics

Several 2-foot-diameter Hermes I lucite rings have experienced over 1000 firings with no damage. Similar cast-epoxy rings have performed well for about 500 firings with some minor dendriting. The Hermes II tube was tested in several configurations. First a lucite tube with a 4-foot outside diameter was tested in 72- and 88-inch lengths. The tube presently being used is an epoxy unit which has no sharp protrusion into the insulator body; the complete unit is shown in Fig. 13.

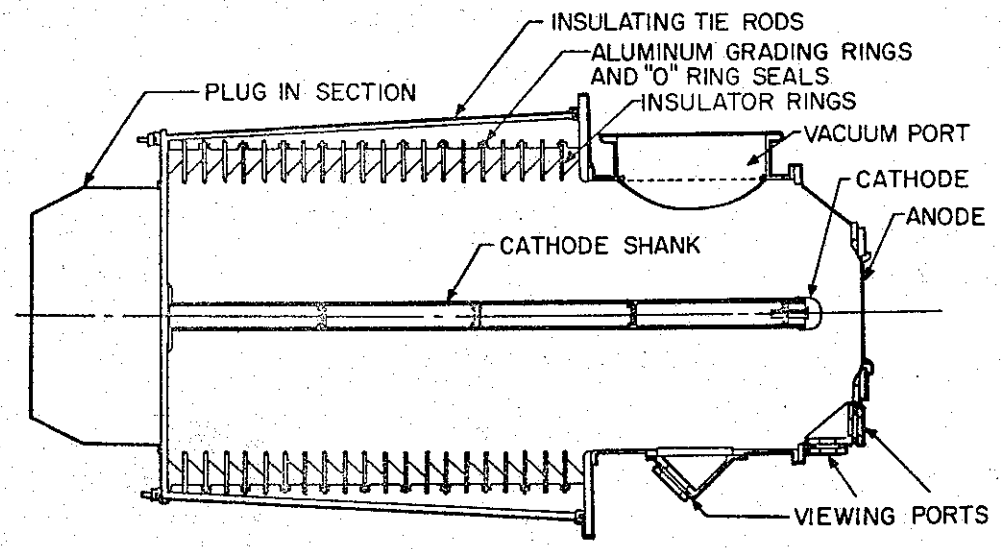

Fig. 13 Hermes II epoxy tube.

Severe dendriting occurred on the lucite tube at all sharp internal corners of the insulator. This included O-ring and metal grading ring grooves. All intrusions into the epoxy tube were eliminated by extending the grading rings through the epoxy into the oil and using captive O-ring grooves in the grading rings.

Tube insulator flashover occurs when the tube voltage exceeds the surface breakdown level of the vacuum side of the tube. No damage is apparent when this occurs, but this phenomenon determines the maximum voltage that can be placed across the tube. Tube flashover data are shown in Table 4.

These breakdown data can be approximately described by the function

$$Ft_{eff}^{1/6} d^{1/10} = 550 ,$$

where F is the flashover field in kilovolts per inch, t_{eff} is in nanoseconds, and d is in inches. This function was first hypothesized at AWRE based on data available for tubes having a 2-foot diameter and operated under 5 MV. In the Hermes II tube this maximum level was never again achieved on the same tube. Typically, these levels of flashover should be reduced by 20 percent under multishot conditions.

TABLE 4

Tube Flashover Data

Tube material	Total insulator length (in.)	Max. V before flashover (MV)	F (kV/in.)	$Ft_{eff}^{1/6}\, d^{1/10}$
Hermes I:	effective time, 90 nsec			
Lutice	20.6	4.3	210	600
Epoxy	20.6	4.3	210	600
Hermes II:	effective time, 100 nsec			
Lucite	62.0	9.4	156	510
Lucite	75.5	12.2	161	535

Hermes II Transfer Efficiency

The lumped constant circuit shown in Fig. 14 approximates the Hermes II machine during the transfer of energy from the Marx to the Blumlein. The symbols in Fig. 14 represent the following:

C_m = series capacity of the Marx = 5.4×10^3 pF

R_s = equivalent series resistance of the Marx

L_T = total series inductance of Marx, Blumleins, and connecting wires = 80 μH

R_P = total parallel resistance formed by dc charging resistors and monitor resistors = 14.4×10^3 Ω

C_{B1} = outer Blumlein capacity and equivalent stray capacities = 3.4×10^3 pF

C_{B2} = inner Blumlein capacity = 1.8×10^3 pF

L_I = isolation inductor and feedthrough to inner Blumlein = 6.5 μH

V_m = Marx capacitor voltage

V_B = Blumlein transmission line voltage

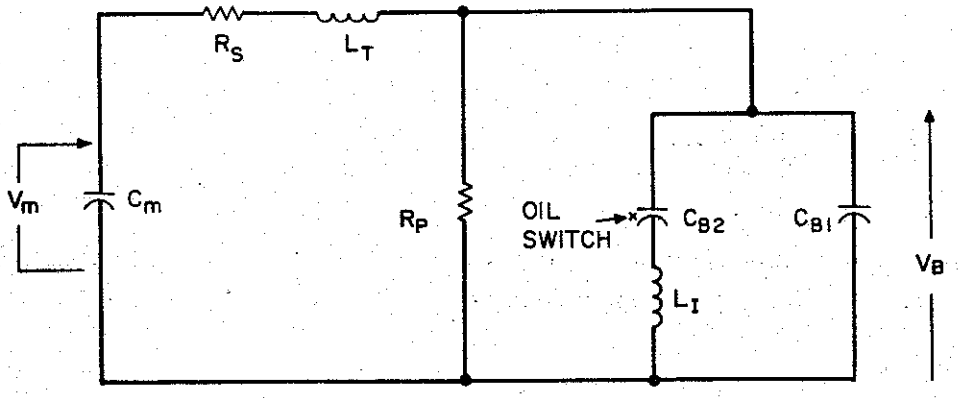

Fig. 14 Approximate Hermes equivalent circuit.

As a first approximation to provide a simple solution to this circuit in the region of interest, it is known that the normalized voltage waveshapes shown in Fig. 15 are approximately obtained across the Marx and Blumlein capacities. Symbols used in Fig. 15 are as follows:

$$T_o = \pi\sqrt{L_T C_{eq}} \quad = \text{time of peak voltage on the Blumlein,}$$

$$C_{eq} = \frac{(C_m)(C_{B_1} + C_{B_2})}{C_m + C_{B_1} + C_{B_2}} ,$$

$$CG = \frac{2C_m}{C_{B_1} + C_{B_2} + C_m} .$$

By assuming these voltages are cosine functions and solving for the energy loss in the resistors, the following approximation is obtained:

$$G = \sqrt{\frac{CG^2 - \frac{\pi}{\omega}\frac{R_S}{L_T}\left(\frac{C_m}{C_m + C_B}\right)}{1 + \frac{0.75\,\pi}{\omega C_B R_P}}} ,$$

where

$$G = \frac{V_B}{V_m} \quad \text{at } T_o$$

and

$$\omega = 1/\sqrt{L_T C_{eq}} \quad .$$

By substituting these values into the equations, the following results are obtained which are then compared to the measured values:

$G_{meas} = 0.81$, $G = 0.826$

Voltage losses due to series R = 10 percent

Voltage losses due to parallel R = 5 percent

Voltage losses due to stray capacities ≈ 5 percent

The formula was also verified with good results on the Hermes I machine which has significantly different parameters.

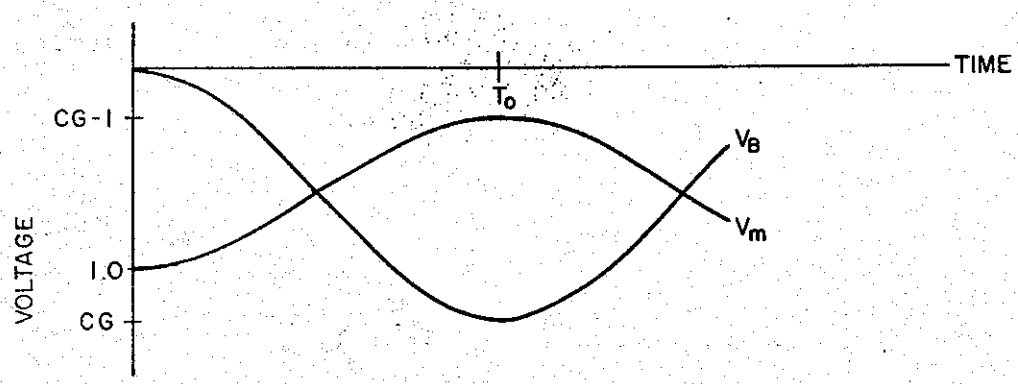

Fig. 15 Time-dependent lossless Blumlein and Marx charge voltages.

The actual energy transferred in both machines is, of course, somewhat less since the Blumlein switch should fire at about 0.9 of the peak voltage to prevent arcing due to the time dependence of the oil breakdown ($F\ t^{1/3}$).

The theoretical Blumlein open circuit voltage gain is 2. This gain is degraded by three main factors: voltage rise time caused by the inductance of the Blumlein switch and the tube cathode shank, the isolating inductor feedthrough to the center Blumlein, and the tube voltage monitor resistor. These losses have been calculated by Thévein's equivalent circuit as applied to transmission lines and the following results shown in Table 5 are obtained.

TABLE 5

Blumlein Losses

Item	Voltage losses (%)
Voltage rise time	10.5
Charging inductor	4.2
Monitor resistor (1000 Ω)	3.4
Predicted open circuit gain, 1.63	
Measured open circuit gain, 1.63	

Mismatch between the output impedance of the Blumlein and the tube impedance causes further minor losses. The tube impedance is typically 70 Ω, thus giving an energy efficiency of

$$\eta = \frac{136\ Z_T}{(34 + Z_T)^2} = 0.88\ .$$

Collecting the above efficiencies, we find the overall efficiency. Converting the primary energy store to electron beam energy is approximately

$$\eta_{\text{total for machine}} = 0.30.$$

Prepulse and Prepulse Effects

Early in the testing of Hermes I erratic tube behavior occurred. The problem was characterized by low tube impedance and unrepeatable spatial distribution of the electron stream. The cause of this was isolated to a voltage (or prepulse) which is applied to the tube prior to the main voltage pulse.

One possible equivalent circuit for the Hermes II x-ray generator is shown in Fig. 16. The 1800-pF capacitor representing the inner Blumlein transmission line must be isolated from ground by an inductor, since it becomes the high-voltage terminal during discharge of the transmission line. The voltage appearing across the isolating inductor during charging of the transmission line also appears across the x-ray tube. This voltage, called the prepulse voltage, is detrimental to the operation of the x-ray tube.

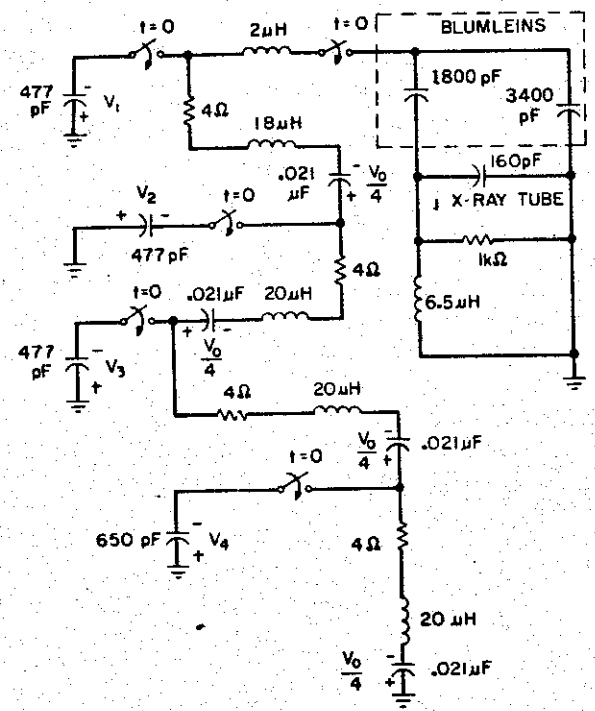

Fig. 16 Hermes II equivalent circuit.

Hermes II voltage traces are shown in Figs. 17 and 18. The oscillating voltage preceding the main pulse is the prepulse voltage.

The circuit shown in Fig. 16 was analyzed on an analog computer. This study showed that increasing the voltage across the stray capacities from the high-voltage end of the Marx to ground would increase the prepulse voltage from 3 to 18 percent of the Marx output voltage. One way that the voltage across the strays could be varied in the x-ray machine was to change the location of the trigger gaps. Experiments on the machine showed that much lower amplitude prepulses were present if the triggers were located 8 rows back from the high-voltage end of the generator. Figure 18 shows a voltage trace with a small prepulse voltage. It was hypothesized that this prepulse voltage causes plasmas to form inside the tube. The plasmas then act as electron sources during the main pulse. Thus the apparent geometrical shape of the cathode was not the electron-emitting shape during the main pulse.

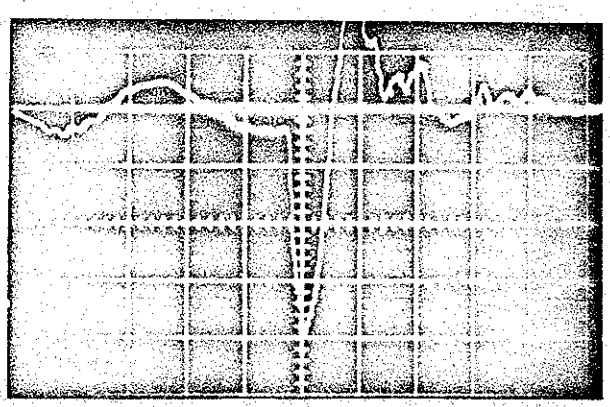

Output voltage

Fig. 17 Hermes II x-ray tube voltage trace (large prepulse, 1.6 MV/cm, 200 nsec/cm).

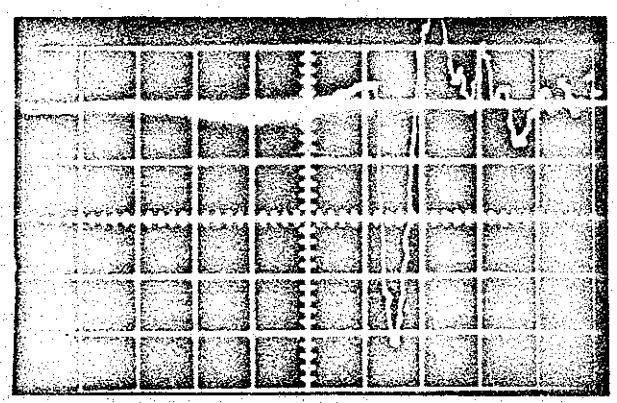

Output voltage

Fig. 18 Hermes II x-ray tube voltage pulse (small prepulse, 1.6 MV/cm, 200 nsec/cm).

As a verification of this hypothesis, an experiment was conducted to determine the approximate voltage level at which the plasma formation occurred. A Marx generator capable of generating 500-kV pulses with an approximate time period of 0.3 μsec was assembled and operated across the Hermes I x-ray tube. An impedance of 1000 Ω in the anode-cathode gap could be detected by the recorded voltage measurements. Data consisted of voltage measurements across the tube and photographs of the anode-cathode gap. Other parameters were tube pressure and cathode configuration. During the experiment the time coincidence between the voltage trace and the plasma glow was verified by a streak camera. A typical anode-cathode gap of approximately 3 inches was used for these experiments. A summary of the data is given in Table 6. The scaled cathode shapes are shown in Fig. 19.

TABLE 6

Voltage Levels at Onset of
Prepulse Plasmas for Various Cathodes

Cathode type	A-K gap (in.)	Tube pressure, (torr x 10^4)	Avg. BD volts (kV)	t_{eff} (μsec)
Single sharp needle	2-3/4	3.5	180	0.3
Multipoint sharp needles	3	3.6	180	0.3
Blunt single needle	3	4.0	250	0.3
Round Lucite insert	3	2.3	170	0.4
Long Lucite cathode	2-3/4	2.5-10	No BD at 455 kV	> 2.0
Hemisphere end	2-3/4	2.8	No BD at 460 kV	> 2.0

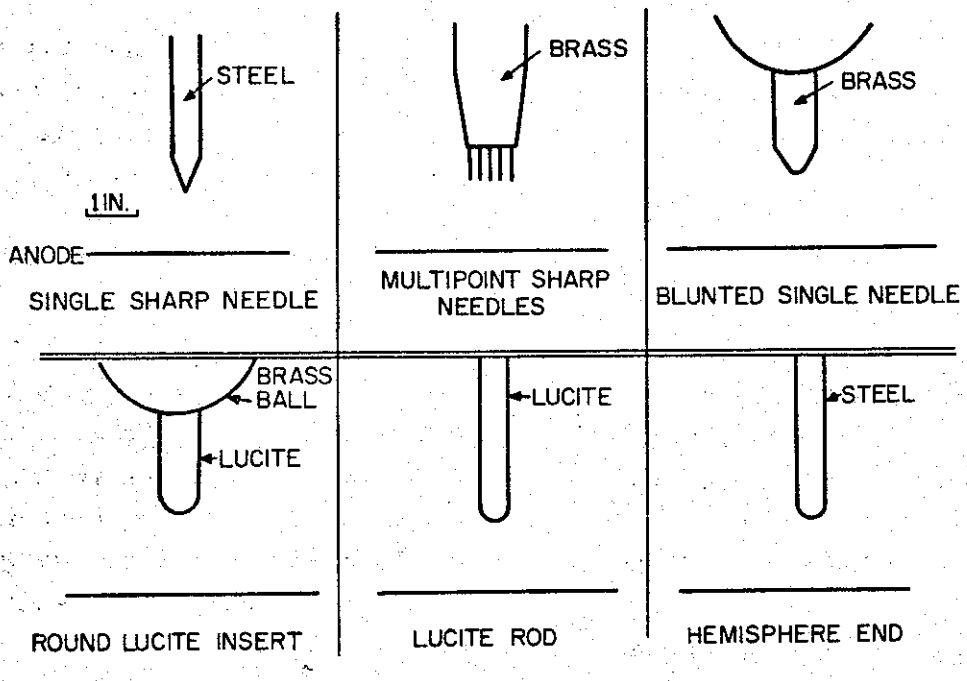

Fig. 19 Cathodes used for prepulse experiments.

Conclusions from these tests were:

1. In time periods and voltages similar to those occurring in low-inductance Marx x-ray machines, considerable ionization can occur in the anode-cathode gap which distorts the apparent electron-emitting shape of the cathode. Only a negative pulse was used on these experiments. The prepulse actually alternates polarity, and lower breakdown voltages could occur during actual machine operation.

2. There exists at least a factor of 3 in the breakdown voltage between sharp pointed and smooth blunt cathodes.

3. Short, blunt Lucite cathodes ionize at levels similar to sharp, pointed metal rods.

In subsequent experiments on the Hermes machines a simple hemispherical tipped or blunt cathode has been utilized to minimize plasma formations. The elimination of these plasmas has allowed analysis of the electron trajectories with the use of a computer code written and modified by J. E. Boers.[12] A simple result has been obtained from this complicated computer program which relates the steady-state tube

impedance to simple geometric parameters. If the cylindrical container of the blunt cathode has a diameter of b, the blunt cathode has a nominal cylindrical diameter of a, and the anode-cathode spacing is approximately a or greater, the tube impedance is given approximately by

$$Z_T = 30 \ln b/a ,$$

or one-half the equivalent coax line impedance. This result was found to be fairly independent of anode-cathode spacing over a limited range, tube pressure, and blunt cathode shape. Actual effects of anode-cathode spacing with a 6-inch-diameter hemispherical cathode at voltage levels of 8 to 10 MV are shown in Fig. 20. In addition, the computer program predicts a halo-type distribution of electrons across the target surface which is also observed (see Fig. 24). Typical computer electron trajectories in the anode-cathode region are shown in Fig. 21.

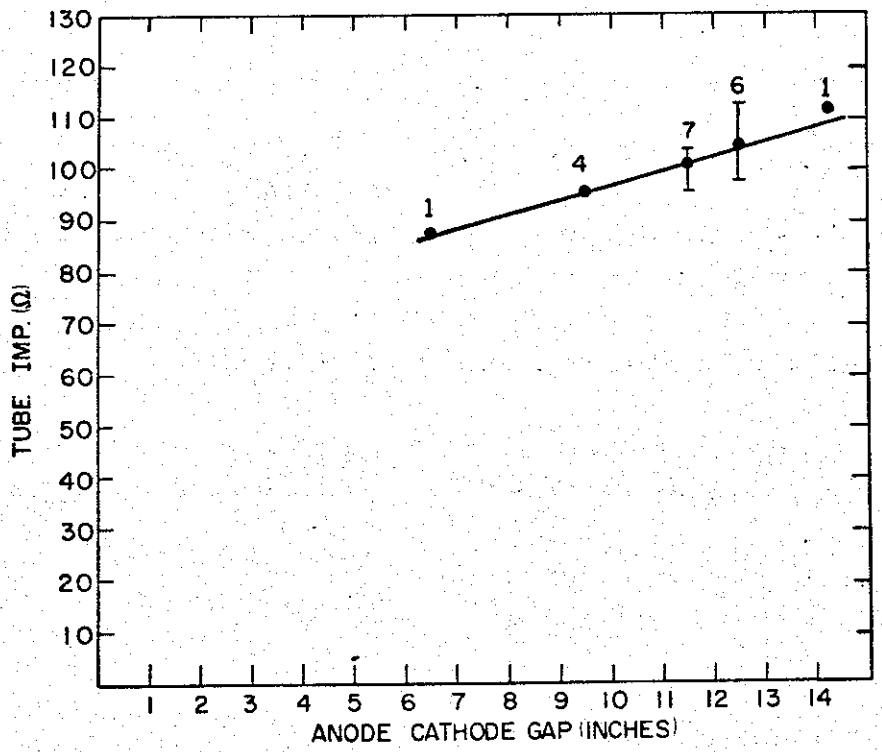

Fig. 20 Hermes II data-tube impedance versus anode-cathode gap.

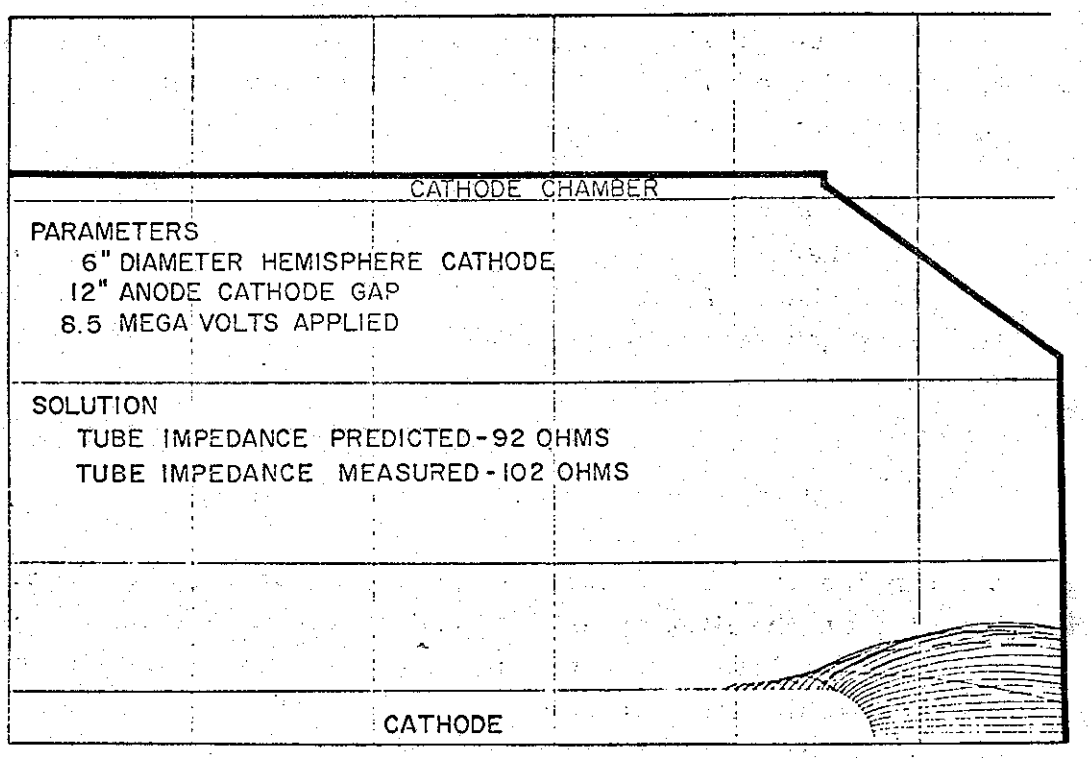

Fig. 21 Computer-calculated Hermes II electron trajectories.

Another important phenomenon occurs when electrons are emitted from the cathode shank. In practice, the shank appears to emit electrons readily. Electrons emitted along the shank can be trapped by the magnetic fields caused by the currents in the anode-cathode gap or be accelerated by the electric field into the cathode chamber sides. A reasonably accurate derivation of this trapping mechanism can be made by finding the condition where the electric field force equals the magnetic field force on a relativistic electron between the cathode shank and its container. One finds that this occurs when

$$Z_T = 60 \ln b/a ,$$

where

Z_T = the impedance of the anode-cathode gap,

b = the outer container diameter,

and

a = the cathode shank diameter.

If Z_T is less than 60 ℓn b/a, the emitted shank electrons return rapidly and are essentially confined to the shank area by the magnetic field. If Z_T is greater than 60 ℓn b/a, the shank electrons cross the tube and strike the container walls, lowering the apparent tube impedance and sometimes causing damage. Thus, given a ratio of diameters between an emitting cathode shank and its container, the upper bound on tube impedance is established. This relationship places limitations on future large flash x-ray generators unless some circumvention of the problem can be found.

Postpulse and Postpulse Suppression

The postpulse as defined here is the transient voltage occurring in the Blumlein, in the Marx generator, and in the tube after the main voltage pulse is completed. The postpulse arises from remaining energy in the Marx and Blumleins. Similar voltage transients also occur during most unintentional voltage sparkovers such as the Blumlein or tube shorting to ground. Voltage breakdown of insulators between capacitor stages in the high-voltage end of the Hermes II Marx generator occurred and was attributed to the postpulse. An investigation of this phenomenon was initiated. A review of documented firings on Hermes I and Hermes II showed interesting patterns. From analysis of a typical firing the tube appeared to be shorting at about 0.4 μsec after the main pulse. When this short occurred, the Marx generator experienced severe voltage transients and, at times, the anode of the tube was destroyed. A model circuit was designed to test methods of rapidly dissipating the remaining Marx and Blumlein energy before this anode-cathode short occurred. The most effective method found was to provide an oil spark gap that connects the center Blumlein feed inductor to a grounded resistor after the main pulse. The resistor impedance must equal the impedance of the outer Blumlein. The location of the spark gap and resistor are diagrammed in Fig. 22. These components were added to the Hermes I and the anode and cathode damage greatly decreased. In turn, this produced a more repeatable electron beam output. A similar modification was made to Hermes II and after several test firings showed no damage to either the target or to the Marx generator insulators at levels exceeding those where damage had occurred. Effective dissipation of the stored energy was obtained even during subsequent fault modes. The resistor will cause energy

losses in the machine if the oil switch breaks down early, and care must be taken to set the switch gap. All of the high radiation shots conducted on Hermes II were conducted with this modification.

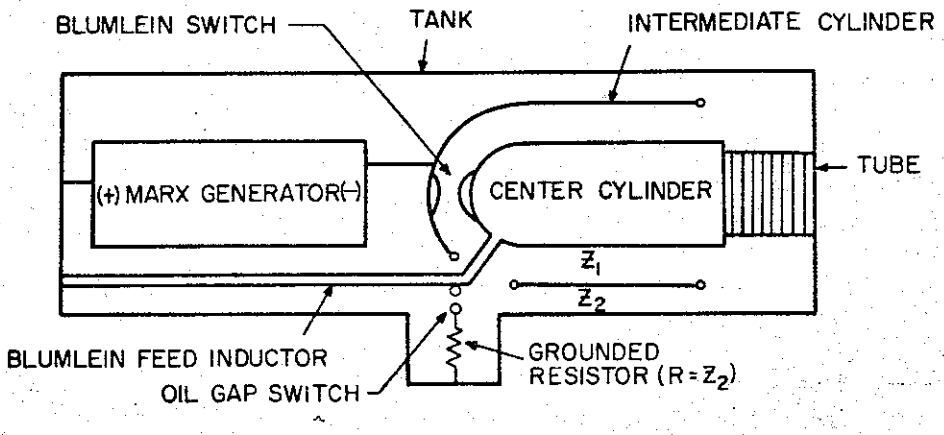

Fig. 22 Hermes electrical diagram.

HERMES II OUTPUT SUMMARY

One method of achieving reliable operation in high-voltage equipment is to establish the maximum output of the machine and then decrease the voltage for routine operation. The results presented here represent the establishment of this maximum level.

The maximum output achieved to date has been 6000 rads (H_2O) at 1 meter with a tube voltage of 12 million volts, an estimated current of 150 kA, and a radiation pulse width of 70 nsec.

The radiation angular distribution at 1 meter is measured by thermoluminescent dosimeters. A typical radiation distribution is shown in Fig. 23. This distribution is then compared with a computer program to determine the average electron arrival angle.[13] With the geometries tested, electron streams with a few degrees of convergence or divergence were achieved in the low prepulse experiments.

A typical radiation profile across the tube face as measured by silver phosphate glass is shown in Fig. 24. The halo pattern is evident.

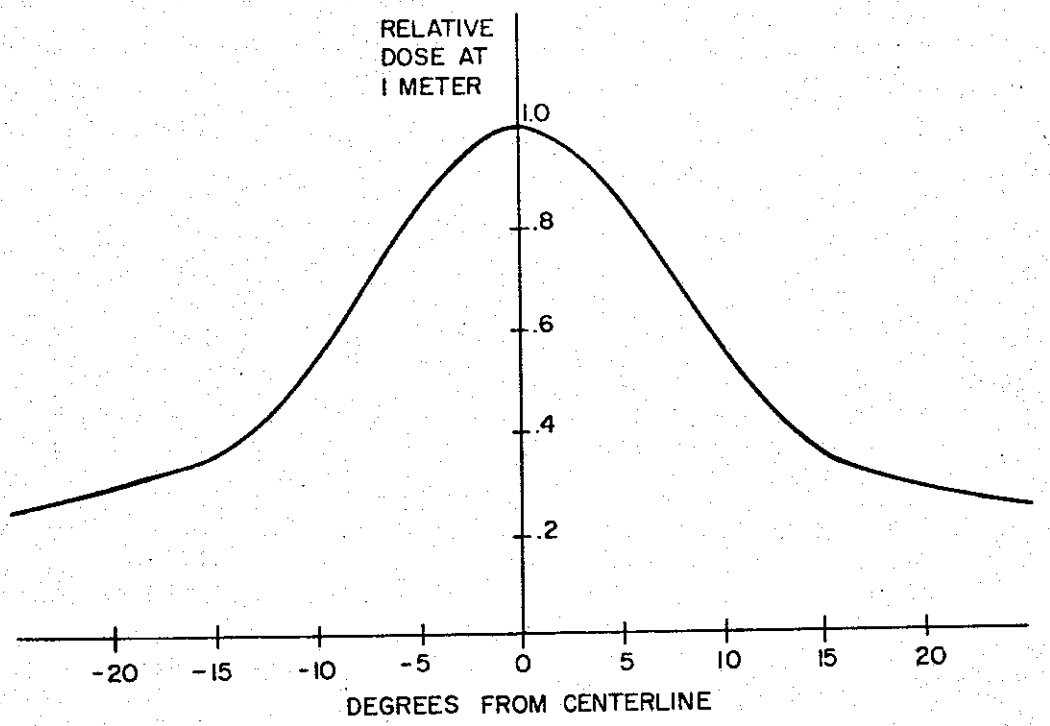

Fig. 23 Typical radiation distribution.

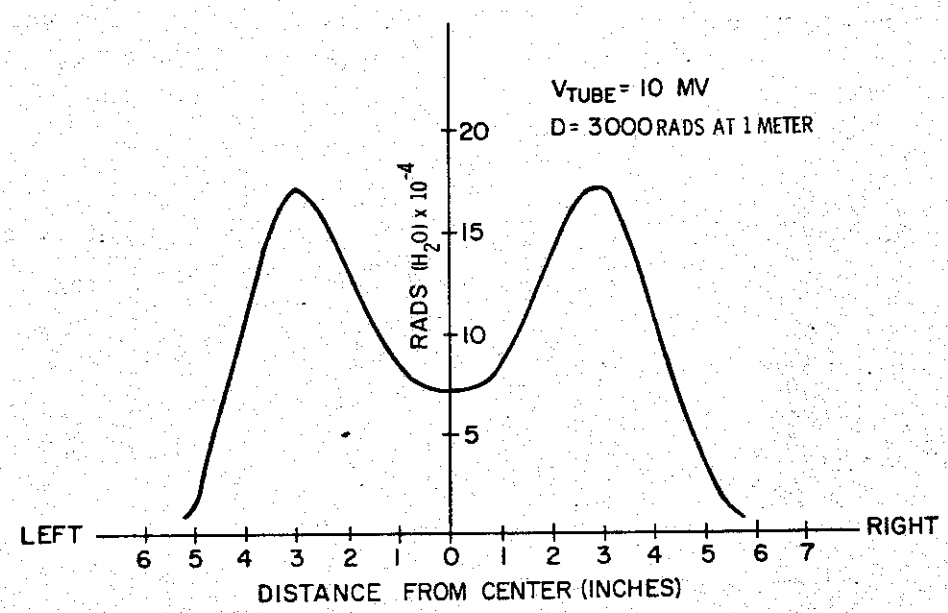

Fig. 24 Typical radiation levels across Hermes II target surface.

The normal operating level of Hermes II for extended life is now being established and preliminary data give the following results in Table 7 for the operational condition.

TABLE 7

Present Hermes II Operational Level

Dose at 1 meter (rads, H_2O)	4000
Dose at 3/4 meter (rads, H_2O)	8000
Dose at 1/2 meter (rads, H_2O)	17000
Tube voltage	10 MV
Radiation pulse half-width	70 nsec

REFERENCES

1. W. T. Link, "Electron Beams from 10^{11} - 10^{12} Watt Pulsed Accelerators," IEEE Transactions on Nuclear Science, Vol. NS-14, No. 3, 777, June 1967.

2. S. E. Graybill and S. V. Nablo, "The Generation and Diagnosis of Pulsed Relativistic Electron Beams Above 10^{10} Watts," IEEE Transactions on Nuclear Science, Vol. NS-14, No. 3, 782, June 1967.

3. F. M. Charbonnier, J. P. Barbour, J. L. Brewster, W. P. Dyke, and F. J. Grundhauser, "Intense, Nanosecond Electron Beams," IEEE Transactions on Nuclear Science, Vol. NS-14, No. 3, 789, June 1967.

4. W. T. Link and D. H. Sloan, "10^{12}-Watt Electron Beam," Record of IEEE 9th Symposium on Electron, Ion, and Laser Beam Technology, 77, May 1967.

5. W. P. Dejhe, J. P. Barbour, F. J. Grundhauser, and F. M. Charbonnier, "An Electron Accelerator with a Peak Beam Power of 10^{10} Watts," Proceedings of the 8th Annual Electron and Laser Beam Symposium, 505, April 1966.

6. B. H. Bernstein, Pulsed X-ray Prompt Gamma Simulator, Technical Report No. BSD-TR-66-386, November 1966.

7. H. Aslin, D. Sloan, et al., Feasibility Analysis of Advanced Power Concentrators, AFWL-TR-66-119, Vol. 1, Kirtland AFB, New Mexico, August 1967, page 8.

8. I. D. Smith, "Pulse Breakdown of Insulator Surfaces in a Poor Vacuum," Proceedings of the International Symposium on Insulation of High Voltages in Vacuum, 261, Oct. 19-21, 1964.

9. J. D. Craggs and J. M. Meek, High Voltage Laboratory Technique (Butterworths Scientific Publications) London, 1954, Chap. 4.

Circuit and Electromagnetic System Design Note 10

10. J. C. Martin, AWRE, private communication.

11. D. Dandy, AWRE, private communication.

12. J. E. Boers, Computer Simulation of Space-Charge Flows, RADC-TR-68-175, University of Michigan, April 1968.

13. T. H. Martin, A Computerized Method of Predicting Electron Beam Bremsstrahlung Radiation with Specific Application to High Voltage Flash X-Ray Machines, SC-RR-69-241, Sandia Laboratories, May 1969.

Radiation Production Note 2